BALKAN PHYSICS LETTERS
© Bogazici University Press 16 April 2009
BPL, **16** (1), pp. 173 - 182, 161030 (2009)

FINAL RESULTS ON $\nu_\mu \rightarrow \nu_\tau$ OSCILLATION FROM THE CHORUS EXPERIMENT

Roumen Tsenov
Department of Atomic Physics, St. Kliment Ohridsky University of Sofia,
BULGARIA.

On behalf of the CHORUS Collaboration.

(received 14 December 2008 ; accepted 14 December 2008)

Abstract. - Brief description of the CHORUS apparatus, data taking, reconstruction algorithms and the final oscillation analysis of the complete set of data collected in the years 1994–1997 is presented. In a two-neutrino mixing scheme, a 90% C.L. upper limit of $sin^2 2\theta_{\mu\tau} < 4.4 \times 10^{-4}$ is set for large Δm^2, improving by a factor 1.5 the previously published CHORUS result.

1. Introduction

The CHORUS experiment was designed to search for $\nu_\mu \rightarrow \nu_\tau$ oscillations through the observation of charged-current interactions $\nu_\tau \; N \rightarrow \tau^- X$ followed by the decay of the τ lepton, directly observed in a nuclear emulsion target. The experiment aimed at achieving maximum sensitivity on the effective mixing angle for values of the mass parameter Δm^2 larger than $10 \; eV^2/\mathrm{c}^4$. This particular choice was based on the hypothesis that the neutrino mass could contribute to the solution of the Dark Matter puzzle [1]. A short-baseline experiment in the CERN SPS Wide Band Neutrino Beam was well suited for this search.

The CHORUS experiment took data from 1994 to 1997. A first phase of data analysis ('Phase I') was performed and no evidence for oscillations was found [2, 3]. Owing to several improvements in automated emulsion scanning and in the event reconstruction, it was considered worthwhile to perform more complete analysis of the data collected in the 1996–1997 period ('Phase II'). Results published recently [4] have led to an improvement of the CHORUS sensitivity to $\nu_\mu \rightarrow \nu_\tau$ appearance by a factor 1.5 and to $\nu_e \rightarrow \nu_\tau$ appearance by a factor 1.2.

In this talk we describe briefly the CHORUS apparatus and data collection, followed by

some details about the event reconstruction and principles of the analysis. Then we give the final CHORUS results on upper limits for $\nu_\mu \rightarrow \nu_\tau$ and $\nu_e \rightarrow \nu_\tau$ oscillations.

Although it is now established that $\nu_\mu \rightarrow \nu_\tau$ oscillations occur at $\Delta m^2 \sim 10^{-3} eV^2/\mathrm{c}^4$, we try to show here the capabilities of an hybrid emulsion experiment and that the goal for which CHORUS was designed has been reached.

2. The experimental setup

The experiment was performed in the CERN Wide Band Neutrino Beam, which consists essentially of ν_μ with a contamination of about 5.1% $\overline{\nu}_\mu$, 0.8% of ν_e, and 0.2% of $\overline{\nu}_e$, while the flux of ν_τ is negligible [5]. The average neutrino energy is 26 GeV, well above the τ production threshold.

The CHORUS detector (Fig. 1) is a hybrid setup which combines a nuclear emulsion target with various electronic detectors such as trigger hodoscopes, a scintillating fiber tracker system, a hadron spectrometer, electromagnetic and hadronic calorimeters, and a muon spectrometer. Brief description of the subdetectors is given below and more details could be found in [6] and references therein.

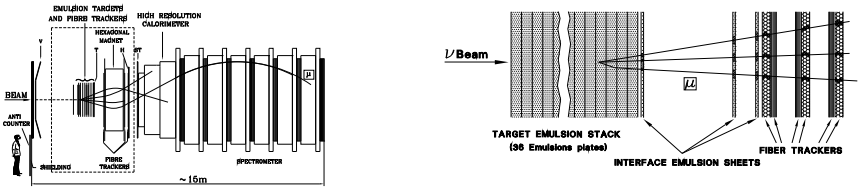

Figure 1: General layout of the detector together with layout of an emulsion stack and associated fiber trackers.

Neutrino interactions occur in a target of nuclear emulsions, whose spatial resolution (below one μm) allows a precise three dimensional *visual* reconstruction of the neutrino interaction vertex as well as of the decay vertices of associated short-lived particles. It is a powerful detector technique to directly observe τ decays which, in this experiment, occur on average at a distance of 1.7 mm from the interaction vertex. The experiment is sensitive to most of the decay channels of the τ.

The emulsion target has an overall mass of 770 kg and is segmented into four stacks. Each stack consists of 8 modules with 36 plates of size 36 cm$\times$71 cm. Each plate has a 90 μm plastic base coated on both sides with a 350 μm emulsion layer. Each stack is followed by three interface emulsion sheets having a 100 μm emulsion layer on both sides of a 800 μm thick plastic base, and by a set of target tracker planes made of scintillating fibers with 500 μm diameter. The target tracker predicts particle trajectories on the interface emulsion sheets with

a precision of about 150 μm in position and 2 $mrad$ in track angle. The layout of an emulsion stack is sketched in Fig. 1.

The emulsion scanning is performed by computer-controlled, fully automated microscope stages each of them equipped with a CCD camera and a read-out system called 'track selector' [7]. The last generation of automated microscopes used in CHORUS experiment is the UTS ('Ultra Track Selector') [8]. In order to recognize track segments in the emulsion, a series of tomographic images is taken by focusing at different depths in the emulsion layer. The digitized images at different depths are shifted according to the predicted track angle and then added. The presence of aligned grains forming a track is detected as a local peak in the gray-level of the summed image. The track-finding efficiency is higher than 98% for track slopes less than 400 $mrad$ [7].

Downstream of the target region, a magnetic spectrometer performs the reconstruction of charge and momentum of charged particles. An air-core magnet of hexagonal shape produces a pulsed homogeneous field of 0.12 T. Field lines are parallel to the sides of the hexagon and the magnetized region extends for a depth of 75 cm in the direction of the beam. The tracking before and after the magnet is performed by another tracker made of scintillating fibers of the same type and complemented with few planes of electronic detectors (streamer tube chambers in the 1994, 1995 and the beginning of 1996 runs, honeycomb chambers afterwards). The resulting momentum resolution $\Delta p/p$ is 30% at 5 GeV. In addition to the detection elements described above, the air-core hexagonal magnet region has been equipped with emulsion trackers for the 1996 and 1997 runs. The aim was to perform a more precise kinematical analysis of the τ decay candidates.

A 100 ton *spaghetti* calorimeter made of lead and scintillating fibers follows the magnetic spectrometer and measures the energy and direction of electromagnetic and hadronic showers. The calorimeter is followed by a muon spectrometer made of magnetized iron disks interleaved with plastic scintillators and tracking devices. A momentum resolution of 19% is achieved by magnetic deflection for muons with momenta greater than 7 GeV. At lower momenta, the measurement of the range yields a 6% resolution.

During the 4 years of operation the emulsion target has been exposed to the neutrino beam for an integrated intensity which corresponds to 5.06×10^{19} protons on target. The data acquisition system recording the response of the electronic detectors was operational for 90% of the time. The average dead time for the emulsion interaction triggers was 12%. The trigger efficiency was 99% for charged current (CC) and 90% for neutral current (NC) events.

3. Principle of the analysis, event reconstruction and decay search

The search for ν_τ interactions has been performed for the following decay modes of the τ lepton: $\tau^- \to \mu^- \nu_\tau \bar{\nu}_\mu$, $\tau^- \to h^-(n\pi^0)\nu_\tau$, $\tau^- \to h^+h^-h^-(n\pi^0)\nu_\tau$. These decay modes give rise in the emulsions to a $kink$ topology: a track from the neutrino interaction vertex showing a change in direction after a short path of the order of 1 mm.

The information of the electronic detectors has been used to define two data sets, the 1μ and 0μ samples, distinguished by the presence or absence of a reconstructed muon of negative charge. For each sample few kinematical selections are applied to reduce the scanning load,

while keeping a high sensitivity to the decay modes of the τ.

An event belongs to the 1μ **sample** if it contains one reconstructed muon track of negative charge. The muon identification and reconstruction is based on the muon spectrometer response. Muons not reaching the spectrometer can in some cases be identified in the calorimeter. Momentum and charge are then measured, with lower precision, by the air-core magnet (for stopping muons the momentum is obtained from the range). The efficiency for selecting of such events is about 80% and is the product of the efficiency for muon identification and that of the track and vertex reconstruction algorithms. The resulting 1μ sample consists of 713000 events. The data set to be analyzed for the search of τ decays was defined by the requirement that the event contains only one muon, with negative charge and momentum smaller than 30 GeV. The 30 GeV selection reduces by 29% the number of events to be scanned.

The 0μ **sample** contains events where no muon is found. Events are selected if tracks have been reconstructed by the scintillating fiber trackers and the reconstructed vertex position lies in the target emulsions. This sample consists of 335000 events, with a calculated contamination of about 140000 misidentified CC interactions and about 20000 interactions generated by neutrinos other than ν_μ.

The **event reconstruction** starts with the pattern recognition in the electronic detectors. Tracks are found in the target tracker, in the calorimeter and in the muon spectrometer. Vertices are reconstructed by the electronic detectors using the points of closest approach of the tracks in the tracker planes immediately downstream from the target. The main vertex is the most upstream one and is selected if it contains either a muon or a hadron surviving criteria which differed in the two phases [1] . Such particles or the muon are used as so-called 'scan-back' tracks. The impact points of the scan-back tracks are predicted on the most downstream interface emulsion sheets, to initiate their follow back in the emulsion.

The event reconstruction in emulsion starts with a procedure called 'vertex location'. As a first step, all the tracks in the interface emulsion sheets within an area of 1 mm^2 centred on each scan-back track prediction are collected. Then, emulsion tracks are associated with the tracks found in the target tracker based on position and direction matching. Once an emulsion track is associated to a scan-back track it is followed upstream from one emulsion plate to the next within a greatly reduced scanning area (a square of 50 μm side) as the resolution improves. The scan-back procedure stops when a searched track is not found in two consecutive plates. The most downstream one is defined as the 'vertex plate'.

The negative track, hadron or muon, selected as a candidate for τ daughter has to satisfy further requirements. To allow the good functioning of the automatic scanning systems, the angle of the track with the beam axis has to be smaller than 400 $mrad$. In view of the large background of muons originating from a nearby secondary beam, tracks at an angle smaller than 50 $mrad$ from the direction of this beam are also excluded (this selection was only applied on 1994 and 1995 data when the secondary beam was run at high intensity). After all selections the 1μ and the 0μ data sets eligible for emulsion scanning consist of 477600 and 122400 events respectively. The events sent to the automatic scanning procedure are

[1] For 0μ events in Phase I at least one hadron with a momentum less than 20 GeV$/c$ was required. In Phase II the most isolated hadron was selected regardless of its charge and momentum.

Table 1: Data flow chart

Protons on target	5.06×10^{19}
1μ: events with 1 negative muon and vertex predicted in emulsion	713000
1μ: $p_\mu < 30$ GeV and angular selections	477600
1μ: events scanned	355395
1μ: vertex located	143742
1μ: events selected for eye-scan	11398
0μ with vertex predicted in emulsion (CC contamination)	335000 (140000)
0μ with 1 negative track (p = 1-20 GeV and angular selections)	122400
0μ: *NetScan*-ned events	102544
0μ: vertex plate found	35039
0μ: *NetScan* acquisition accepted	29404
0μ: vertex reconstructed	22661
0μ: events selected for visual inspection	754

fewer mainly because of fiducial volume cuts imposed by the scanning technique and of the bad quality of a few emulsion plates. The different stages of the reconstruction and selection procedure are summarized in Table 1.

The reconstruction inefficiencies, as well as those originating from the trigger, are well understood and reproduced by detailed MC simulations, both for the 1μ and the 0μ data sets.

Once the vertex plate is defined, automatic microscope measurements are performed to select the events potentially containing a decay topology (kink). Different algorithms have been applied as a result of the progress in the scanning procedures and of the improving performance in speed of the scanning devices.

For most of the 1μ **events** the vertex plate is assumed to contain the decay vertex of a charged parent produced in a more upstream plate. The upstream part of the vertex plate is scanned in order to find a track crossing, within a small tolerance, the direction of the daughter candidate as sketched in Fig. 2. The method also works for events where the decay vertex and the primary vertex occur in the same plate but on opposite sides of the plastic base. A computer assisted eye-scan is performed for all the kink candidates selected during the automatic search. The aim of the eye-scan is to confirm the presence of a secondary vertex. An event is retained as a τ^- decay candidate if the secondary vertex appears as a kink without black prongs, nuclear recoils, blobs or Auger electrons. For the selected events the parent and decay particle, as well as the other tracks coming from the interaction vertex, are accurately measured.

The maximum of the sensitivity is obtained through a compromise between low background and high efficiency for ν_τ detection. To illustrate that efficiency, the last column of Table 2 also displays $N_\tau^{\nu_\mu}$, the number of events with ν_τ CC interaction in the emulsion which would be observed in case all incident ν_μ had converted into ν_τ. For the 1μ sample this number is given by:

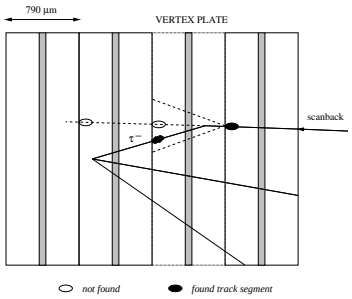

Figure 2: Schematic view of the decay search technique applied for most of the 1μ events. The dotted lines indicate the cone around the scan-back track in which the search for the parent track is performed.

$$(N_\tau^{\nu_\mu})_{1\mu} = N_{1\mu}^{loc} \cdot r_\sigma \cdot r_A \cdot \epsilon_{kink} \cdot Br_\mu,$$

where: $N_{1\mu}^{loc}$ is the number of located 1μ events ($N_{1\mu}^{loc} = 143742$) ; $r_\sigma =< \sigma_\tau^{CC} > / < \sigma_\mu^{CC} >$ is the neutrino energy weighted CC cross-section ratio. A value $r_\sigma = 0.53$ has been used, it takes into account quasi-elastic interactions, resonance production and deep inelastic reactions; $r_A =< A_\tau > / < A_\mu >$ is the cross-section weighted acceptance ratio for ν_τ and ν_μ interactions. A_τ and A_μ take into account the effect of geometrical and kinematical selections applied before scanning and the reconstruction and location efficiencies. The values of r_A is close to one (r_A = 0.97); ϵ_{kink} includes the efficiency of the decay search procedure and that of the geometrical and kinematical selections applied after the kink is found. Its average value is 0.39; $Br_\mu = 17.4\%$ is the branching ratio of the decay $\tau \rightarrow \nu_\tau \bar{\nu}_\mu \mu^-$.

Most of the 0μ **located events** have been reanalyzed in the Phase II of the analysis exploiting the so-called NetScan technique. Originally developed for the DONUT experiment [9], this technique is described in detail in Ref. [10] together with the event location procedure. It is briefly outlined in the following paragraphs [2] .

After identifying the vertex plate, the UTS performs a scan of the emulsion volume around the vertex position, recording, for each event, all track segments within 400 $mrad$ with respect to the orthogonal direction of the plates. In each plate only the most upstream 100 μm part is scanned. The scanned volume is 1.5 mm $\times$ 1.5 mm wide and 6.3 mm long in the beam direction, corresponding to 8 emulsion plates. This volume contains the vertex plate itself, the plate immediately upstream, and the six plates downstream the vertex plate. The plate upstream the vertex acts as a veto for passing through tracks. The six plates downstream from the vertex act as decay volume and are used to detect the tracks of the decay daughters. The scan area is centred on the scan-back track stopping point.

[2]The NetScan technique has been used also for the 1μ data sample, mainly to search for charmed particles decays [11].

The number of track segments (coming from particles induced by neutrino interactions, cosmic ray particles and muons from neighboring beams) found in each plate depends on the position of the NetScan volume with respect to the beam center and on average is 920.

After rejection of isolated track segments based on dedicated alignment procedure, typically about 400 tracks remain in the volume. The majority of these are tracks (mainly Compton electrons and δ-rays) with a momentum less than 100 MeV$/c$. These background tracks are rejected on the basis of the χ^2 of a straight-line fit to the track segments. The final step is the rejection of the tracks not originating from the scan volume. After this filtering, the average number of remaining tracks is about 40. The number of connected tracks and the position and slope residuals provide a good measurement of the alignment quality. About 84% of the events passes the quality cuts ('NetScan acquisition accepted').

The reconstruction algorithm then tries to associate the tracks to vertices with a 'pair-based' method: after selecting pairs of tracks having minimal distance less than 10 μm, a clustering among them is performed and vertex points are defined. After this clustering, a track is attached to a vertex if its distance from the vertex point (called 'impact parameter') is less than 3 μm. At the end of the procedure, one defines a primary vertex (and its associated tracks) and one or more secondary vertices to which 'daughter tracks' are attached.

About 77% of the events, where the NetScan acquisition was accepted, have a vertex reconstructed in the NetScan volume. The loss is accounted for by the fact that a background track might have been selected for the scan-back procedure. The number of events at the various stages of the procedure are given in Table 1.

Once tracks and vertices are reconstructed in the NetScan volume, a search for decay topologies is performed. In Fig. 3 a sketch of a ν_τ Monte Carlo event inside the NetScan volume is shown: a ν_τ (not drawn) interacts producing a τ lepton and other particles. After three plates, the τ lepton decays producing one charged particle (kink topology, *i.e.* an observed abrupt change of direction in the track).

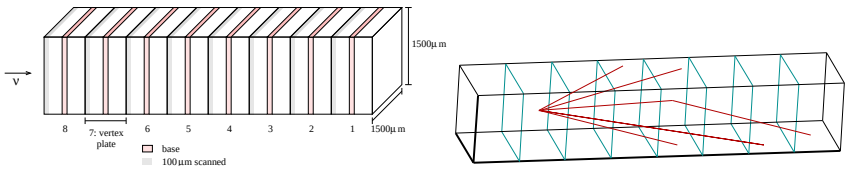

Figure 3: The NetScan volume and a Monte Carlo event with one-prong (*i.e.* kink) τ decay.

The decay search is done by an automated search on the whole sample and then by a computer-assisted visual inspection on the sample selected in the automated search aiming at clear establishing of the topology of the primary and secondary vertices found. After the automated search, 754 events have been selected for inspection.

Decays of the τ lepton are characterized by either one or three charged particles in the final state, *i.e.* they belong to a *C1 topology* when there is a track with a kink (interaction or decay) of at least 50 $mrad$, or to a *C3 topology* where a track produces (via decay or

interaction) three prongs . 59 *C1* events and 48 *C3* events have been found after the visual inspection.

4. Background evaluation

An unavoidable background to $\nu_\mu \rightarrow \nu_\tau$ oscillation is caused by the presence of prompt ν_τ's in the neutrino beam. Calculations show that it is small compared to other sources of background. For the statistics collected by CHORUS it amounts to less than 0.1 events and has been neglected. Apart from this, the background is constituted by any event having a negative track undergoing a deviation of its trajectory or producing several new tracks at some point in the emulsion target. To obtain a realistic estimation of the number of events expected in absence of an oscillation signal, large samples of all the known background processes have been simulated and processed by the same reconstruction programs as the real data.

Table 2 shows the number of simulated (*Background*) and observed (*Data*) events in Phase I and Phase II data samples. The Phase I data consists of the 1μ events from the full data taking period (1994–1997) and a relatively small sample of 0μ one-prong events from the 1994–1995 data taking. The Phase II data consists of 0μ one-prong (*C1 topology*) and three-prong (*C3 topology*) events from the 1996–1997 data taking analyzed with the NetScan technique.

Table 2: The final CHORUS data sample. The first two rows refer to the Phase I analysis, namely to the 1μ channel of the whole data taking (1994–1997) and to a small 0μ sample collected in 1994–1995 and not accounted for in Table 1. The Phase II sample, consisting of the 0μ data collected in 1996–1997 and *NetScan*-ned, is divided in C1 and C3 topologies. For each subsample the following quantities are shown: the expected background; the maximum detectable number of τ events, $N_\tau^{\nu_\tau}$ and $N_\tau^{\nu_e}$ respectively from the ν_μ and ν_e beam components; the number of data events.

Category	Background	$N_\tau^{\nu_\mu}$	$N_\tau^{\nu_e}$	Data
$\tau \rightarrow 1\mu$ $[1994-1997$ data taking$]$	0.100 ± 0.025	5014	55.8	0
$\tau \rightarrow 0\mu$ one negative track $[1994-1995$ data taking$]$	0.300 ± 0.075	526	5.85	0
$\tau \rightarrow 0\mu$ C1 topology $[1996-1997$ data taking$]$	53.2 ± 9.0	9621	76.9	59
$\tau \rightarrow 0\mu$ C3 topology $[1996-1997$ data taking$]$	47 ± 11	4443	35.5	48

The errors on the expected background are evaluated by taking into account the limited statistics of the Monte Carlo sample and the errors on cross-sections and branching ratios.

5. Results

From the number of observed candidates, the expected background and the number of signal events expected for full oscillation it is possible to compute the 90% C.L. upper limit on the

ν_τ appearance probability using a frequentist statistical approach, the so-called Feldman and Cousins unified approach [12].

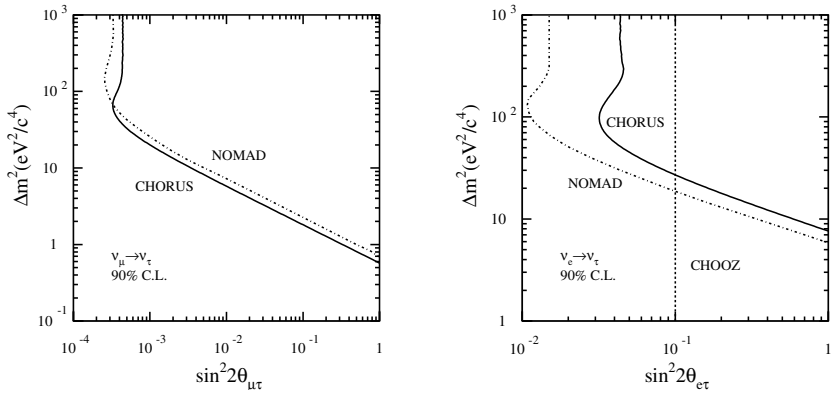

Figure 4: The CHORUS upper limit on $\nu_\mu \to \nu_\tau$ (left) and $\nu_e \to \nu_\tau$ (right) oscillation represented in an exclusion plot in the oscillation parameter plane. CHORUS results are shown as solid lines and are compared with the final results of NOMAD [13] and CHOOZ [14].

The 90% C.L. upper limit on the ν_τ appearance probability obtained from the data is

$$P(\nu_\mu \to \nu_\tau) < 2.2 \times 10^{-4}.$$

It is in agreement with the expected sensitivity. The result improves by a factor 1.5 the limit $P < 3.4 \times 10^{-4}$ based on the Phase I analysis only [3].

In a two-neutrino formalism, the above upper limit corresponds to the exclusion region in the (Δm^2, $sin^2 2\theta_{\mu\tau}$) oscillation parameter plane shown in Fig. 4 (left) and to the limit $sin^2 2\theta_{\mu\tau} < 4.4 \times 10^{-4}$ for large Δm^2.

Another experiment, NOMAD, used the same beam and searched for ν_τ appearance using a purely electronic technique [13]. The upper limit obtained by NOMAD is more stringent than the CHORUS one at large Δm^2, whereas for Δm^2 lower than 70 eV^2/c^4 the upper limit is improved by CHORUS owing to its higher efficiencies at low neutrino energies.

The SPS neutrino beam contains a 0.8% ν_e contamination. Assuming that all observable ν_τ would originate from this contamination, the above result translates into a limit on the $\nu_e \to \nu_\tau$ appearance probability. The difference in energy between the ν_μ ($\langle E_{\nu_\mu} \rangle \sim 26$ GeV) and ν_e ($\langle E_{\nu_e} \rangle \sim 42$ GeV) components leads to a smaller ν_τ detection efficiency and different shape of the exclusion plot in the oscillation parameter plane.

The 90% C.L. upper limit on the appearance probability obtained from the data is $P(\nu_e \to \nu_\tau) < 2.2 \times 10^{-2}$. It improves by a factor 1.2 the Phase I limit [3]. In a two-neutrino

formalism, the obtained upper limit corresponds to the exclusion region shown in Fig. 4 (right) and to the limit $sin^2 2\theta_{e\tau} < 4.4 \times 10^{-2}$ for large Δm^2.

Acknowledgments

The author gratefully acknowledges the support of the organizers of the International Conference on Particle Physics 2008 in Istanbul and of the Swiss National Science Foundation and the Swiss Agency for Development and Cooperation within the framework of the programme SCOPES, that made his participation in the conference possible.

REFERENCES

[1] H. Harari, *Phys. Lett.* **B216** (1989) 413,
J. Ellis, J.L. Lopez and D.V. Nanopoulos, *Phys. Lett.* **B292** (1992) 189.
[2] E. Eskut *et al.*, CHORUS Collaboration, *Phys. Lett.* **B424** (1998) 202,
E. Eskut *et al.*, CHORUS Collaboration, *Phys. Lett.* **B434** (1998) 205.
[3] E. Eskut *et al.*, CHORUS Collaboration, *Phys. Lett.* **B497** (2001) 8.
[4] E. Eskut *et al.*, CHORUS Collaboration, Nucl. Phys. A **783** (2008) 326.
[5] B. Van de Vyver and P. Zucchelli, *Nucl. Instr. and Meth.* **A385** (1997) 91.
[6] E. Eskut *et al.*, CHORUS Collaboration, *Nucl. Instr. and Meth.* **A401** (1997) 7.
[7] S. Aoki *et al.*, *Nucl. Instr. and Meth.* **B51** (1990) 466,
T. Nakano, Ph.D. thesis, Nagoya University, Japan (1997).
[8] T. Nakano, Proc. Int. Europhys. Conf. on High Energy Physics, Budapest (2001).
[9] K. Kodama *et al.*, *Nucl. Instr. and Meth.* **A493** (2002) 45.
[10] N. Nonaka, Ph.D. thesis, Nagoya University, Japan (2002), M. Güler, Ph.D. thesis, METU, Ankara, Turkey (2000), L. Scotto Lavina, Ph.D. thesis, Universitá degli Studi di Napoli "Federico II" (2005).
[11] G. Onengut *et al.*, CHORUS Collaboration, *Phys. Lett.* **B613** (2005) 105,
G. Onengut *et al.*, CHORUS Collaboration, *Phys. Lett.* **B614** (2005) 155.
[12] G.J. Feldman and R.D. Cousins, *Phys. Rev.* **D57** (1998) 3873.
[13] P. Astier *et al.*, NOMAD Collaboration, *Nucl. Phys.* **B611** (2001) 3.
[14] M. Apollonio *et al.*, CHOOZ Collaboration, *Eur. Phys. J.* **C27** (2003) 331.